

# 000 001 002 003 004 005 006 007 008 009 010 011 012 013 014 015 016 017 018 019 020 021 022 023 024 025 026 027 028 029 030 031 032 033 034 035 036 037 038 039 040 041 042 043 044 045 046 047 048 049 050 051 052 053 RHGCL: REPRESENTATION-DRIVEN HIERARCHICAL GRAPH CONTRASTIVE LEARNING FOR USER-ITEM RECOMMENDATION

006 **Anonymous authors**

007 Paper under double-blind review

## 010 ABSTRACT

013 Graph Contrastive Learning (GCL), which fuses graph neural networks with con-  
014 trastive learning, has evolved as a pivotal tool in user-item recommendations.  
015 While promising, existing GCL methods often lack explicit modeling of hierar-  
016 chical item structures, which represent item similarities across varying resolu-  
017 tions. Such hierarchical item structures are ubiquitous in various items (e.g., on-  
018 line products and local businesses), and reflect their inherent organizational prop-  
019 erties that serve as critical signals for enhancing recommendation accuracy. In this  
020 paper, we propose Representation-driven Hierarchical Graph Contrastive Learn-  
021 ing (RHGCL), a novel GCL method that incorporates hierarchical item structures  
022 from learned representations for recommendations. First, RHGCL pre-trains a  
023 GCL module using cross-layer contrastive learning to obtain user and item rep-  
024 resentations. Second, RHGCL employs a representation compression and clus-  
025 tering method to construct a two-hierarchy user-item bipartite graph. Ultimately,  
026 RHGCL fine-tunes user and item representations by learning on the hierarchical  
027 graph, and then provides recommendations based on user-item interaction scores.  
028 Experiments on three widely adopted benchmark datasets ranging from 70K to  
029 382K nodes confirm the superior performance of RHGCL over existing baseline  
030 models, highlighting the contribution of representation-driven hierarchical item  
031 structures in enhancing GCL methods for recommendation tasks.

## 032 1 INTRODUCTION

033 Graph Contrastive Learning (GCL) represents a key branch of methods in recommendation systems,  
034 with notable models such as SGL (Wu et al., 2021a), SimGCL (Yu et al., 2022), and SGRL (He et al.,  
035 2024). GCL integrates graph neural networks (GNNs), which capture collaborative signals within  
036 user-item graphs (He et al., 2020), with contrastive learning (Chen et al., 2020; Grill et al., 2020),  
037 a self-supervised approach that generates representations based on positive and negative sample  
038 pairs (Ju et al., 2024; Lin et al., 2022). Since GCL retains the self-supervised representation learning  
039 capability, it is advantageous for recommendation systems where supervised signals are sometimes  
040 sparse. As examples of GCL, researchers have utilized information bottleneck principles to design  
041 graph contrastive modules (Xu et al., 2021a). Besides, user prompts derived from user profiles have  
042 been used to enhance GCL-based recommendation frameworks (Yang et al., 2023). Following these  
043 methods, various experiments conducted on widely adopted datasets, such as Gowalla (Cai et al.,  
044 2023), MovieLens (Lin et al., 2022), and Yelp (Yu et al., 2023a), have demonstrated the superiority  
045 of GCL for recommendation tasks.

046 However, existing GCL-based recommendation methods are still limited. Although certain GCL-  
047 based recommendation approaches consider heterogeneous graphs where nodes exhibit various  
048 types (Wang et al., 2021b), they ignore hierarchical structures inherent within items in user-item  
049 graphs. Here, hierarchical item structures refer to organizations of items with analogous properties  
050 at distinct resolutions. For instance, snooker videos and football videos can be categorized under  
051 the broader class of sports videos, while sports videos and music audio can be grouped as general  
052 entertainment products. Effectively mining these hierarchical dependencies among items can extract  
053 valuable item signals for recommendation in two ways. First, the system enables multi-level rec-  
ommendations, as it could recommend items that are either directly related in the original user-item

graph or exhibit similarity within a broader category (Qin et al., 2023). Second, it effectively mitigates data sparsity issues, because it can recommend items with a few interaction records through the transfer of information from higher-level categories that contain abundant interaction data. Unfortunately, there exists a scarcity of generalizable GCL methods that effectively model hierarchical item structures for user-item recommendation tasks from the following aspects (See Appendix A for more details).

- Recent seminal models GraphLoG (Xu et al., 2021b) and HIGCL (Yan et al., 2023) have incorporated hierarchical item structures for general GCL tasks, rather than focusing on user-item recommendations.
- DiffPool (Ying et al., 2018b) and HiGNN (Li et al., 2020) have highlighted the central role of hierarchical item structures, but not in the context of GCL for recommendations.
- Knowledge graph-based GCL methods, such as HEK-CL (Yuan et al., 2025a) and HKGCL (Liang et al., 2018), rely on knowledge relationships between items to perform recommendation. Despite their effectiveness, a practical barrier to their widespread adoption is the high cost required to construct and maintain up-to-date knowledge graphs.
- Existing representation clustering methods such as NCL (Lin et al., 2022) and HNECL (Wei et al., 2025) apply contrastive learning between node representations and their clustered prototype representations. This tends to reduce embedding uniformity, which is a property shown to be beneficial for prediction performance in graph contrastive learning (Yu et al., 2023a).

In this study, we propose Representation-driven Hierarchical Graph Contrastive Learning (RHGCL), which incorporates hierarchical item structures into GCL for recommendation systems. Specifically, we first obtain user and item representations by pre-training a graph contrastive learning model on user-item graphs, utilizing a weighted combination of prediction loss and contrastive loss. Afterwards, RHGCL compresses item node embeddings and clusters item nodes, thereby constructing user-cluster item graphs. Finally, we derive ultimate user and item embeddings by fine-tuning the model on both the original user-item graphs and the newly user-clustered item graphs. **To preserve the uniformity of item node embeddings, we do not include clustered item representations in contrastive learning at this stage.** To access the contribution of hierarchical item structures, we conduct experiments comparing RHGCL with state-of-the-art GCL methods, including SGL (Wu et al., 2021a), SimGCL (Yu et al., 2022), and XSimGCL (Yu et al., 2023a), on three publicly available recommendation datasets comprising 70K, 237K, and 382K nodes. The recommendation performance, as indicated by Recall and NDCG scores, demonstrates the superior performance of our RHGCL model.

## 2 RELATED WORK

### 2.1 GRAPH NEURAL NETWORKS FOR RECOMMENDATION

Recommendation systems provide personalized recommendations to web users based on their preferences (Davidson et al., 2010; Kang & McAuley, 2018). Such systems require robust capabilities for learning from complicated user-item interactions (Feng et al., 2025; Lin et al., 2025). These interactions can be seamlessly modeled by GNN methods (Kipf, 2016; Hamilton et al., 2017; Gao et al., 2023), including GCNs (Ying et al., 2018a), NGCF (Wang et al., 2019), and RDL (Robinson et al., 2024). Subsequently, LightGCN simplified NGCF by discarding redundant linear transformation and nonlinear activation functions in NGCF (He et al., 2020). As a pioneering practice, PinSage integrates GNNs with customized random walk-based information fusion for recommendations on Pinterest (Ying et al., 2018a). Recently, OmniSage extended PinSage by combining graph-based relation modeling, sequence-based evolution modeling, and content-based information fusion (Badrinath et al., 2025). In addition to efficient information propagation, node compression emerges as another viable solution in GNNs for recommendation. Notably, LiGNN, developed by LinkedIn, models various entities including members, posts, and jobs as a giant graph (Borisuk et al., 2024). The used techniques include adaptive multi-hop neighborhood sampling, training data grouping and slicing, and shared-memory queues. Besides, MacGNN aggregates user and item nodes with analogous behavior into macro nodes and learns their representations, supporting online product recommendations on Taobao’s homepage (Chen et al., 2024a).

108  
109

## 2.2 GRAPH CONTRASTIVE LEARNING FOR RECOMMENDATION

110  
111  
112  
113  
114  
115  
116  
117  
118  
119  
120

GCL constitutes an unsupervised learning approach that constructs representations from graph data (Veličković et al., 2018). The general process involves creating multiple graph views through graph perturbations (e.g., node deletion, edge modifications, and subgraph sampling), with the strategy of maximizing node representation consistency across these views (You et al., 2020). It facilitates the learning of intrinsic graph structure properties that remain invariant under these perturbations (Zhu et al., 2020). While initial GCL models contain graph perturbation operations, GraphACL discards graph perturbations and leverages one-hop and two-hop neighborhood nodes to develop node representations (Xiao et al., 2023). Recently, GCFormer enhances graph Transformers (Wu et al., 2021b) by incorporating contrastive signals from positive and negative node tokens relative to a target node, exhibiting its superiority over conventional graph Transformers in node classification applications (Chen et al., 2024b).

121  
122  
123  
124  
125  
126  
127  
128  
129  
130

The self-supervision capability of GCL is well-suited to mine user-item interactions in user-item recommendation systems (Yu et al., 2023b). Specifically, SGL refines supervised user-item graph learning with the contrastive loss (e.g., the InfoNCE loss (Oord et al., 2018)), to improve recommendation accuracy and robustness (Wu et al., 2021a). This seminal work has inspired subsequent GCL methods for recommendation. For example, HCCL integrates local and global collaborative signals within user-item graphs through hypergraphs (Xia et al., 2022). Heterogeneous GCL incorporates heterogeneous relational semantics within graphs (Chen et al., 2023). Another approach, LightGCL, optimizes graph augmentations by applying singular value decomposition to facilitate local and global contrastive learning (Cai et al., 2023). Additionally, industrial researchers have addressed the challenge posed by the long-tail distribution of node degrees by creating pseudo-tail nodes in GCL for recommendation (Zhao et al., 2023).

131  
132  
133  
134  
135  
136  
137  
138

It is worth mentioning that graph augmentations are not invariably indispensable in GCL for recommendation. Empirical studies have revealed that the uniformity of learned representations plays a central factor in GCL for recommendation (Yu et al., 2022). They proposed SimGCL, incorporating additive uniform noise vectors into node representations to enhance representation uniformity. Furthermore, recommendation researchers refined SimGCL into XSimGCL, which reduces the number of forward and backward information propagation steps from three to one (Yu et al., 2023a). This is achieved by unifying recommendation prediction and contrastive learning together, and contrasting node representations across distinct layers within a single neural network.

139  
140

## 3 PRELIMINARIES

141  
142  
143  
144  
145  
146  
147

Following existing studies (Wang et al., 2021a; Yuan et al., 2025b), the user-item recommendation problem is formulated as a link prediction task on a user-item bipartite graph, denoted as  $\mathcal{G} = (\mathcal{V}, \mathcal{E})$ . Here, the node set  $\mathcal{V} = \mathcal{U} \cup \mathcal{I}$  comprises the user set  $\mathcal{U}$  and the item set  $\mathcal{I}$ , where  $m = |\mathcal{U}|$  and  $n = |\mathcal{I}|$  represent the cardinalities of  $\mathcal{U}$  and  $\mathcal{I}$ , respectively. The edge set  $\mathcal{E}$  captures user-item interactions that denote ratings, searches, purchases, and etc. The objective of user-item recommendation is to suggest separate items for each user given observed user-item engagements.

148  
149

## 3.1 GRAPH NEURAL NETWORKS

150  
151  
152  
153  
154  
155

GNNs serve as critical approaches in user-item recommendation systems by learning representations for  $m$  users and  $n$  items:  $\mathbf{E} \in \mathbb{R}^{(m+n) \times d}$ , where  $d$  denotes the embedding dimension. The matrix  $\mathbf{E}$  is derived as the final representation matrix within a sequence of representations  $\mathbf{E}^{(k)}$  where  $0 \leq k \leq K$ . Here,  $K$  signifies the number of layers in the GNN. The information propagation mechanism of a seminal GNN model, LightGCN (He et al., 2020), is expressed as follows:

156  
157  
158

$$\mathbf{E}^{(k+1)} = \mathbf{D}^{-\frac{1}{2}} \mathbf{A} \mathbf{D}^{-\frac{1}{2}} \mathbf{E}^{(k)}, \quad (1)$$

159  
160  
161

where  $0 \leq k \leq (K - 1)$ .  $\mathbf{A}$  is the adjacency matrix of  $\mathcal{G}$ . Besides,  $\mathbf{D}$  denotes the degree matrix of  $\mathcal{G}$ , where  $D_{ll}$  represents the sum of the entries in the  $l$ -th row of  $\mathbf{A}$  ( $1 \leq l \leq m + n$ ). To recommend items to a user  $i$ , we compute the final connecting strength  $\hat{y}_{ij}$  between user  $i$  and an arbitrary item  $j$  as  $\hat{y}_{ij} = (\mathbf{e}_i)^\top \mathbf{e}_j$ , where  $1 \leq i \leq m$ ,  $1 \leq j \leq n$ , and  $\mathbf{e}_i, \mathbf{e}_j \in \mathbb{R}^d$  are embeddings extracted from

162 E. We then recommend items to user  $i$  by ranking  $\hat{y}_{ij}, 1 \leq j \leq n$  in descending order. To train  
 163 the model, we typically adopt the Bayesian Personalized Ranking loss (Rendle et al., 2012) as the  
 164 recommendation loss:

$$\mathcal{L}_{rec} = \sum_{(i,j^+,j^-)} -\log (\sigma(\hat{y}_{i,j^+} - \hat{y}_{i,j^-})) , \quad (2)$$

169 where  $\sigma(\cdot)$  is the sigmoid function, positive edges  $(i, j^+) \in \mathcal{E}$ , and negative edges  $(i, j^-) \notin \mathcal{E}$ . This  
 170 loss facilitates the updating of learnable node representations (i.e.,  $\mathbf{E}^{(0)}$ ) to increase or decrease the  
 171 inner products of endpoint representations associated with positive or negative edges, respectively.  
 172

### 173 3.2 GRAPH CONTRASTIVE LEARNING

175 The intuition behind GCL for recommendation systems is to learn robust and intrinsic user and item  
 176 representations that are invariant under graph perturbations where graph structures change (Hassani  
 177 & Khasahmadi, 2020). This process entails augmenting the original graph  $\mathcal{G}$  to generate two views:  
 178  $\tilde{\mathcal{G}}_1$  and  $\tilde{\mathcal{G}}_2$ , through operations such as removing nodes or edges given predefined probabilities. The  
 179 goal of node representation updates is to maximize representation similarity for the same nodes  
 180 across the two views while minimizing representation similarity of distinct nodes. To achieve this,  
 181 the InfoNCE loss (Oord et al., 2018) is introduced:

$$\mathcal{L}_{cl} = \sum_{i \in \mathcal{B}} -\log \left( \frac{\exp(\text{sim}(\mathbf{e}_{i1}, \mathbf{e}_{i2})/\tau)}{\sum_{j \in \mathcal{B}} \exp(\text{sim}(\mathbf{e}_{i1}, \mathbf{e}_{j2})/\tau)} \right) . \quad (3)$$

186 Here,  $\mathcal{B}$  is a mini-batch.  $\mathbf{e}_{ik}$  and  $\mathbf{e}_{jk}$  ( $k = 1, 2$ ) denote the representations of nodes  $i$  and  $j$  from  
 187  $\tilde{\mathcal{G}}_1$  and  $\tilde{\mathcal{G}}_2$ , respectively.  $\text{sim}(\cdot, \cdot)$  is a similarity function like the cosine similarity function.  $\tau$   
 188 refers to temperature parameter. Practically, the GCL module can be fused with GNN module via  
 189 a hybrid loss  $\mathcal{L} = \mathcal{L}_{rec} + \lambda \mathcal{L}_{cl}$  ( $\lambda > 0$ ). Learning guided by loss  $\mathcal{L}$  enables the generation of  
 190 robust self-supervised node representations that align effectively with supervised signals derived  
 191 from interactions labels. While Eq. 3 represents the complete formulation of GCL, it is noteworthy  
 192 that some exponents (e.g., positive pairs, and graph augmentations) could be omitted to enhance  
 193 performance for specific recommendation tasks (Guo et al., 2023; Yu et al., 2022).

## 195 4 REPRESENTATION-DRIVEN HIERARCHICAL GRAPH CONTRASTIVE 196 LEARNING

197 In this section, we present RHGCL, which performs graph learning on user-item graphs and user-  
 198 clustered item graphs. The underlying intuition is to capture hierarchical structures of item nodes  
 199 while ensuring uniformity of representations.

### 202 4.1 PRE-TRAINING REPRESENTATIONS ON USER-ITEM BIPARTITE GRAPHS

204 During the pre-training stage (Fig. 1, left), RHGCL obtains user and item representations using  
 205 historical user-item interaction records. The objective is to model user and item characteristics  
 206 without considering hierarchical item structures. To achieve this, we resort to XSimGCL (Yu et al.,  
 207 2023a), a state-of-the-art GCL approach in user-item recommendation systems.

208 The model consists of three primary components: (1) graph convolution operator, (2) random noise  
 209 incorporation, and (3) cross-layer contrastive learning. First, the model passes node representations  
 210 using light graph convolution operation (i.e., Eq. 1), which captures collaborative filtering signals  
 211 from user-item interactions. Note that the initial embedding matrix  $\mathbf{E}^{(0)}$  serves as the collection  
 212 of learnable representations of users and items. Second, for layer  $0 \leq k \leq (K - 1)$ , the model  
 213 introduces a random noise vector  $\Delta_i^k$  into the node representations  $\mathbf{e}_i^k$  on the node  $i$ :

$$(\mathbf{e}_i^k)' = \mathbf{e}_i^k + \Delta_i^k, \quad (4)$$

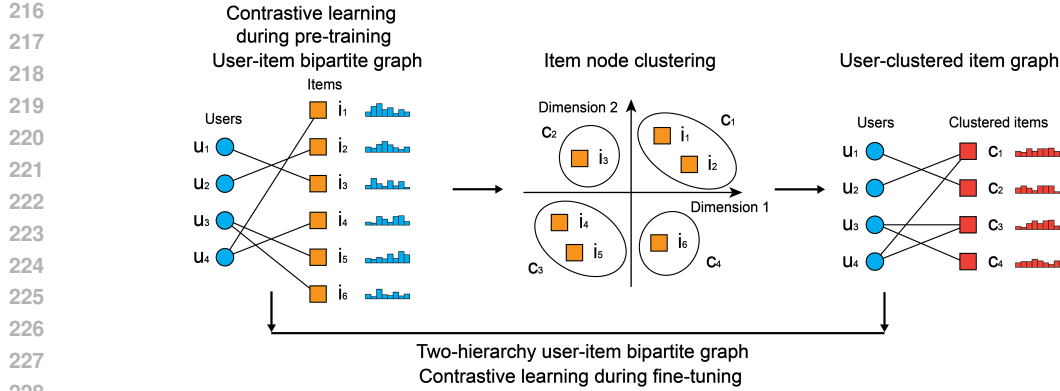


Figure 1: The framework of RHGCL. Initially, RHGCL generates user and item representations using XSimGCL (Yu et al., 2023a), which comprises graph convolution operators with cross-layer contrastive learning (Sec. 4.1). Afterwards, the learned high-dimensional item representations are projected into a two-dimensional latent space using the t-SNE algorithm, forming distinct clusters of item nodes (Sec. 4.2). Building upon these item clusters, RHGCL constructs user-clustered item graphs with clustered items (Sec. 4.3). We then jointly optimize representations of users, items, and clustered items under recommendation and contrastive losses. Finally, RHGCL leverages optimized representations of users, items, and clustered items to infer personalized item rankings for each user.

and propagates  $(\mathbf{e}_i^k)'$  rather than  $\mathbf{e}_i^k$  to the next layer of graph convolution. Here, the length of  $\Delta_i^k$  is set as a predefined hyperparameter  $\epsilon$ :  $\|\Delta_i^k\| = \epsilon > 0$ . The rationale for adding the random noise vector term lies in its capacity to enhance representation uniformity, which improves recommendation performance (Yu et al., 2022). Third, different from Eq. 3, the contrastive learning loss  $\mathcal{L}_{cl}$  is constructed by contrasting node representations across different layers within the same graph convolution network.

$$\mathcal{L}_{cl} = \sum_{i \in \mathcal{B}} -\log \left( \frac{\exp(\text{sim}(\mathbf{e}_i^K, \mathbf{e}_i^{K^*})/\tau)}{\sum_{j \in \mathcal{B}} \exp(\text{sim}(\mathbf{e}_i^K, \mathbf{e}_j^{K^*})/\tau)} \right). \quad (5)$$

Here,  $0 \leq K^* \leq K$  is a hyperparameter, representing the layer used for contrastive learning with the  $K$ -th layer. This ingenious design is theoretically supported by spectral graph analysis for contrastive learning (Yu et al., 2023a). Finally,  $\mathcal{L}_{cl}$  is integrated with the recommendation loss  $\mathcal{L}_{rec}$  to form the hybrid loss  $\mathcal{L}$  (Sec. 3.2). Together, after training the model using information passing (Eq. 1) with added noises (Eq. 4), as well as  $\mathcal{L}$ , we obtain stable pre-trained representations of users as  $\mathbf{E}_{\mathcal{U}}^{pt} \in \mathbb{R}^{m \times d}$  and items as  $\mathbf{E}_{\mathcal{I}}^{pt} \in \mathbb{R}^{n \times d}$ .

## 4.2 CLUSTERING ITEM NODES

After reaching node representations (i.e.,  $\mathbf{E}_{\mathcal{U}}^{pt}$  and  $\mathbf{E}_{\mathcal{I}}^{pt}$ ) from the pre-training stage, the next step of RHGCL is to explicitly model hierarchical item structures. We build these structures by delving into the item similarity (Brovman et al., 2016; Giahi et al., 2023). These item similarity signals play crucial roles in facilitating effective item recommendations for users. For example, a user who has interacted with a basketball video is more likely to prefer a football video over a music audio file. Practically, there are two approaches to evaluate item similarity. First, there exists similarity between two items when they share common attributes (e.g., geolocations, item types). Second, two items are considered similar if they are accessed by similar groups of users and maintain similar node representations (Baltescu et al., 2022). Note that the first approach requires domain-specific attribute information for each user-item recommendation problem, exhibiting weaker generalizability than the second approach. To promote model generalizability, we customize our hierarchical item structures based on the second approach.

**Representation Dimension Reduction.** We first perform the t-distributed Stochastic Neighbor Embedding (t-SNE) algorithm (Van der Maaten & Hinton, 2008) to summarize representations from the

270 pre-training stage (Fig. 1, middle). The reason for employing the t-SNE algorithm is that it projects  
 271 high-dimensional vectors to the low-dimensional latent space, while persevering local neighbor  
 272 relationships<sup>1</sup>. This local neighbor persevering characteristic aligns with representations in recom-  
 273 mendation tasks, wherein interacted user and item nodes have similar representations. It is worth noting  
 274 that Principal Component Analysis is not appropriate here, as it is a linear dimensionality reduction  
 275 method capturing global data variance. In the t-SNE algorithm (Van der Maaten & Hinton, 2008),  
 276 for two vectors  $\mathbf{x}, \mathbf{y} \in \mathbb{R}^{d_1}$ , the projected vectors  $\mathbf{x}', \mathbf{y}' \in \mathbb{R}^{d_2}$  should satisfy the two conditions:  
 277 (1)  $d_2 < d_1$ , (2)  $p_{\mathbf{xy}}$  is close to  $q_{\mathbf{x}'\mathbf{y}'}$ . Here,  $p_{\mathbf{xy}}$  (or  $q_{\mathbf{x}'\mathbf{y}'}$ ) quantifies the probability of neighborhood  
 278 relationship of the two vectors  $\mathbf{x}, \mathbf{y}$  (or  $\mathbf{x}', \mathbf{y}'$ ) in the original space (or the new space).  $p_{\mathbf{xy}}$  (or  $q_{\mathbf{x}'\mathbf{y}'}$ )  
 279 is calculated based on the distance of  $\mathbf{x}$  and  $\mathbf{y}$  (or  $\mathbf{x}'$  and  $\mathbf{y}'$ ) relative to the neighborhoods using a  
 280 Student t distribution:

$$p_{\mathbf{xy}} = \frac{1/(1 + \text{distance}(\mathbf{x}, \mathbf{y})^2)}{\sum_{\mathbf{k}, \mathbf{l}} (1/(1 + \text{distance}(\mathbf{k}, \mathbf{l})^2))}. \quad (6)$$

285 Here,  $\text{distance}(\cdot, \cdot)$  denotes a distance metric, such as the squared Euclidean distance.  $\mathbf{k}, \mathbf{l} \in \mathbb{R}^{d_1}$   
 286 are within the neighborhood of  $\mathbf{x}, \mathbf{y}$ . The number of selected neighborhood is measured by a model  
 287 hyperparameter: perplexity. By optimizing  $\mathbf{x}', \mathbf{y}'$  in the two-dimensional space, we are able to con-  
 288 vert item node representations from  $\mathbf{E}_{\mathcal{I}}^{\text{pt}} \in \mathbb{R}^{n \times d}$  to  $\mathbf{E}_{\mathcal{I}}^{\text{tsne}} \in \mathbb{R}^{n \times 2}$ . **Note that the time complexity**  
 289 **of the t-SNE algorithm is  $\mathcal{O}(n^2)$ . This can be optimized to  $\mathcal{O}(n \log(n))$  from the Barnes-Hut SNE**  
 290 **algorithm (Van Der Maaten, 2013) for large graphs.**

292 **Clustering Item Nodes in the Two-Dimensional Space.** Based on  $\mathbf{E}_{\mathcal{I}}^{\text{tsne}}$ , we now cluster item  
 293 nodes in the two-dimensional space. The goal is to form simple and interpretable item node clusters  
 294 for hierarchical item structures. Given the connection difference between distinct user-item graphs,  
 295 we introduce task-specific hyperparameter  $\rho \geq 1$  and  $\theta \geq 1$  to perform item node clustering. Here,  
 296  $\rho$  and  $\theta$  represent the number of divisions along the radial and angular directions, respectively. The  
 297 item nodes whose two-dimensional representations are located within the same sector are clustered  
 298 into a group. This setting leads to the total number of clusters as  $\rho * \theta$ . For example, in Fig. 1,  
 299 middle panel, there are one radial division ( $\rho = 1$ ) and four angular divisions ( $\theta = 4$ ), leading  
 300 to total  $1 * 4 = 4$  clusters of item nodes. Different from the seminal hierarchical GNN study  
 301 DiffPool (Ying et al., 2018a) with soft clustering, our approach utilizes deterministic clustering for  
 302 item nodes to ensure simplicity and enhance interpretability.

### 303 4.3 FINE-TUNING REPRESENTATIONS ON TWO-HIERARCHY USER-ITEM BIPARTITE 304 GRAPHS

306 After representation compressions and item node clustering, we now build user-clustered item  
 307 graphs (Fig. 1, right). We create the clustered item set  $\mathcal{C}$ , which contains the derived clusters from  
 308 item node clustering. Hence,  $|\mathcal{C}| = \rho * \theta$ . In this way, we have extended our original node set  
 309  $\mathcal{V} = \mathcal{U} \cup \mathcal{I}$  to  $\mathcal{V}^c = \mathcal{U} \cup \mathcal{C}$ . We now delineate edges between nodes in  $\mathcal{U}$  and  $\mathcal{C}$ . Particularly, the user  
 310 node  $u \in \mathcal{U}$  is linked to the clustered item node  $c \in \mathcal{C}$  if and only if the user node  $u$  is connected  
 311 to at least one item node within the cluster represented by  $c$ . For instance, node  $u_2$  is connected to  
 312  $c_1$  in the user-clustered item graph (Fig. 1, right), because  $u_2$  is linked to  $i_2$  in the user-item graph  
 313 (Fig. 1, left), and  $i_2$  is a member of cluster  $c_1$  (Fig. 1, middle).

314 Until now, we have obtained two graphs: the user-item graph (i.e.,  $\mathcal{V}$ ), and the user-clustered item  
 315 graph (i.e.,  $\mathcal{V}^c$ ), which are collectively called the two-hierarchy user-item bipartite graph. We per-  
 316 form graph convolution operators (i.e., Eq. 1) on the two graphs separately, and finally obtain three  
 317 fine-tuned representation matrices:  $\mathbf{E}_{\mathcal{U}}^{\text{ft}} \in \mathbb{R}^{m \times d}$ ,  $\mathbf{E}_{\mathcal{I}}^{\text{ft}} \in \mathbb{R}^{n \times d}$ , and  $\mathbf{E}_{\mathcal{C}}^{\text{ft}} \in \mathbb{R}^{(\rho * \theta) \times d}$ . The final  
 318 connecting strength  $y_{ij}$  between user  $i$  and item  $j$  is defined as:

$$\hat{y}_{ij} = (\mathbf{e}_{\mathcal{U}, i}^{\text{ft}})^\top (\mathbf{e}_{\mathcal{I}, j}^{\text{ft}} + \sum_{1 \leq k \leq \rho * \theta} w_{jk} \mathbf{e}_{\mathcal{C}, k}^{\text{ft}}). \quad (7)$$

323 <sup>1</sup><https://distill.pub/2016/misread-tsne/>

324 Here,  $\mathbf{e}_{\mathcal{U},i}^{ft} \in \mathbb{R}^d$  denotes the  $i$ -th row of  $\mathbf{E}_{\mathcal{U}}^{ft}$ , which corresponds to the user representation. Similarly,  
 325  $\mathbf{e}_{\mathcal{I},j}^{ft} \in \mathbb{R}^d$  represents the  $j$ -th row of  $\mathbf{E}_{\mathcal{I}}^{ft}$ , representing the item representation, and  $\mathbf{e}_{\mathcal{C},k}^{ft} \in \mathbb{R}^d$   
 326 denotes the  $k$ -th row of  $\mathbf{E}_{\mathcal{C}}^{ft}$ , indicating the clustered item representation. The term  $w_{jk}$  denotes  
 327 the clustering membership, where  $w_{jk} = 1$  if the item node  $j$  belongs to cluster  $k$ , and  $w_{jk} = 0$   
 328 otherwise. To train the model, we set the hybrid loss:  
 329

$$\mathcal{L} = \mathcal{L}_{rec}^{ui} + \mathcal{L}_{rec}^{uc} + \lambda \mathcal{L}_{cl}^{ui}. \quad (8)$$

330 Here,  $\mathcal{L}_{rec}^{ui}$  and  $\mathcal{L}_{rec}^{uc}$  represent the recommendation loss on the user-item graph and the user-clustered  
 331 item graph, respectively, while  $\mathcal{L}_{cl}^{ui}$  is the cross-layer contrastive learning loss on the user-item graph.  
 332 Notably, we do not include the contrastive learning term between item representations and clustered  
 333 item representations (i.e.,  $\mathcal{L}_{cl}^{ic}$ ), as it may compromise embedding uniformity. Furthermore, we  
 334 provide that the time complexity of RHGCL is slightly higher than that of XSimGCL, due to the  
 335 incorporation of edges in the user-clustered item graph  $\mathcal{V}^c$  (Appendix E).  
 336

## 337 5 EXPERIMENTS

341 To evaluate the performance of RHGCL, we conduct a series of experiments utilizing three publicly  
 342 available datasets. The target of our experiments is to answer the following questions:  
 343

- 344 • **Q1.** What is the performance of RHGCL in various user-item recommendation tasks?
- 345 • **Q2.** Do our hierarchical item structures enhance model performance?
- 346 • **Q3.** How does the number of cluster divisions (i.e.,  $\rho$  and  $\theta$ ) affect prediction accuracy?

### 348 5.1 EXPERIMENT SETTINGS

#### 350 5.1.1 DATASETS AND BASELINE MODELS

352 We employ three classical user-item datasets<sup>2</sup>: **Yelp2018**, **Amazon-Kindle**, and **Alibaba-iFashion**  
 353 to perform recommendation tasks. These datasets have been extensively used in previous user-item  
 354 recommendation studies (Wang et al., 2019; Yu et al., 2023a; 2022) (See Appendix B for statistics).  
 355 Given that existing model comparisons (He et al., 2020; Yu et al., 2023a) have demonstrated that  
 356 the models Mult-VAE (Liang et al., 2018), NGCF (Wang et al., 2019), and MixGCF (Huang et al.,  
 357 2021) exhibit relatively inferior performance compared to state-of-the-art methods, we select the  
 358 following eight models as baselines: **BUIR** (Lee et al., 2021), **DNN+SSL** (Yao et al., 2021), **Light-**  
 359 **GCN** (He et al., 2020), **NCL** (Lin et al., 2022), **SGL** (Wu et al., 2021a), **SimGCL** (Yu et al., 2022),  
 360 **XSimGCL** (Yu et al., 2023a), and **HNECL** (Wei et al., 2025) (See Appendix C for details).  
 361

#### 362 5.1.2 PARAMETERS

363 For BUIR and DNN+SSL, we resort to implementation outcomes in the existing study (Yu et al.,  
 364 2023a). The hyperparameters for LightGCN, SGL, **NCL**, SimGCL, XSimGCL, and **HNECL** in-  
 365 clude the hidden dimension  $d$ , the number of layers  $K$ , the temperature parameter  $\tau$ , and the learning  
 366 weight associated with the contrastive learning loss  $\lambda$ . To ensure a fair comparison, the hyperpa-  
 367 rameters for the Yelp2018 dataset were configured in accordance with the SELFRRec repository<sup>3</sup>.  
 368 The hyperparameters for the Amazon-Kindle and Alibaba-iFashion datasets were set to align with  
 369 those used in the study XSimGCL (Yu et al., 2023a). For **HNECL**, we set the configuration of hi-  
 370 erarchical prototypes as (2000, 1000, 100). Since our RHGCL method is built upon XSimGCL,  
 371 we keep consistent hyperparameters between XSimGCL and RHGCL (Table 1). Finally, the embed-  
 372 ding dimension  $d$  is set to 64, the batch size to 2048, and the learning rate to 0.0001. To train the  
 373 model, we use the Xavier initialization method (Glorot & Bengio, 2010) and refer to the Adam op-  
 374 timizer (Kingma & Ba, 2014). The maximum number of training epochs is set to 50 for Yelp2018,  
 375 100 for Amazon-Kindle, and 50 for Alibaba-iFashion, respectively. The training and testing time  
 376 of RHGCL on a single CPU is around 20, 40, and 60 hours for Yelp2018, Amazon-Kindle, and  
 377 Alibaba-iFashion, respectively.

<sup>2</sup><https://github.com/Coder-Yu/SELFRRec/tree/main/dataset/>

<sup>3</sup><https://github.com/Coder-Yu/SELFRRec>

378  
 379 Table 1: Hyperparameters in RHGCL.  $K$ : the number of layers;  $K^*$ : the layer selected for  
 380 contrastive learning;  $\lambda$ : the weight for contrastive loss;  $\epsilon$ : the length of added noise vectors;  $\tau$ : temper-  
 381 ature parameter;  $\rho$ : the number of representation divisions along the radial direction;  $\theta$ : the number  
 382 of representation divisions along the angular direction.

Dataset	$K$	$K^*$	$\lambda$	$\epsilon$	$\tau$	$\rho$	$\theta$
Yelp2018	3	1	0.20	0.20	0.15	8	2
Amazon-Kindle	3	1	0.20	0.10	0.20	1	2
Alibaba-iFashion	4	4	0.05	0.05	0.20	4	8

387  
 388  
 389 **5.2 OVERALL PERFORMANCE**  
 390  
 391

392 Table 2: Performance comparison. Note that the performance metrics of BUIR and DNN+SSL  
 393 are sourced from the existing study (Yu et al., 2023a). For the remaining four baseline methods,  
 394 we conduct the experiments using our own computational resources. **We use underlining to denote  
 395 the second-best performance. The reported improvement is calculated based on RHGCL and the  
 396 second-best outcome.**

	Yelp2018		Amazon-Kindle		Alibaba-iFashion	
	Recall@20	NDCG@20	Recall@20	NDCG@20	Recall@20	NDCG@20
BUIR (Lee et al., 2021)	0.0487	0.0404	0.0922	0.0528	0.0830	0.0384
DNN+SSL (Yao et al., 2021)	0.0483	0.0382	0.1520	0.0989	0.0818	0.0375
LightGCN (He et al., 2020)	0.0595	0.0487	0.1900	0.1208	0.0885	0.0410
SGL (Wu et al., 2021a)	0.0677	0.0555	0.2098	0.1324	0.1138	0.0541
<b>NCL (Lin et al., 2022)</b>	<b>0.0674</b>	<b>0.0553</b>	<b>0.1857</b>	<b>0.1147</b>	<b>0.0897</b>	<b>0.0417</b>
SimGCL (Yu et al., 2022)	<u>0.0727</u>	<u>0.0598</u>	0.2031	0.1264	0.1176	0.0561
XSimGCL (Yu et al., 2023a)	0.0726	0.0597	<u>0.2061</u>	<u>0.1324</u>	<u>0.1189</u>	<u>0.0569</u>
<b>HNECL (Wei et al., 2025)</b>	<b>0.0674</b>	<b>0.0554</b>	<b>0.1823</b>	<b>0.1096</b>	<b>0.0976</b>	<b>0.0454</b>
RHGCL	<b>0.0736</b>	<b>0.0605</b>	<b>0.2117</b>	<b>0.1354</b>	<b>0.1194</b>	<b>0.0572</b>
Improvement	+1.2%	+1.2%	+2.7%	+2.3%	+0.4%	+0.5%

408  
 409 To examine the recommendation performance of RHGCL, we present recommendation metrics, Re-  
 410 call@20 and NDCG@20 scores on the testing sets of the three datasets in Table 2. Among the  
 411 **nine** models, BUIR and DNN+SSL yield the lowest Recall@20 and NDCG@20 scores across all  
 412 three datasets. This is because these models have limited capability to capture multi-hop user-item  
 413 similarity within historical interactions. In contrast, LightGCN brings improved prediction perfor-  
 414 mance, as this model retains essential graph convolution operations while eliminating redundant  
 415 linear transformations and nonlinear activations in recommendation tasks. As one of the pioneer-  
 416 ing self-supervised models in graph learning, SGL significantly enhances prediction accuracy. This  
 417 improvement can be attributed to the InfoNCE loss function, which pulls node representations asso-  
 418 ciated with positive samples while pushing those linked to negative samples. **NCL** has considered  
 419 **both the structural and semantic neighbors in contrastive learning, leading to competitive predic-  
 420 tion performance. Compared to NCL, HNECL yields similar model performance. This observation  
 421 aligns with the findings reported in the HNECL paper which shows that increasing the number of  
 422 **hierarchical layers provides little additional improvement (Wei et al., 2025)**. Furthermore, SimGCL  
 423 and XSimGCL exhibit the overall highest Recall@20 and NDCG@20 scores among baseline mod-  
 424 els. This achievement is supported by their ability to promote representation uniformity through  
 425 added noise vectors.**

426 Notably, our proposed RHGCL model attains the highest Recall@20 and NDCG@20 scores among  
 427 the **nine** models, highlighting its superior capability in modeling user-item relationships in recom-  
 428 mendation tasks (Answer **Q1**). Recall that RHGCL is an extension of XSimGCL, incorporating  
 429 hierarchical item structures. Hence, the performance comparison between RHGCL and XSimGCL  
 430 further substantiates the beneficial contribution of hierarchical item structures in user-item recom-  
 431 mendation (Answer **Q2**). This conclusion is further confirmed in Appendix D, where we reveal  
 432 that positive user-item pairs exhibit greater distinguishability from negative user-item pairs after  
 433 fine-tuning compared to the distinguishability observed after pre-training.

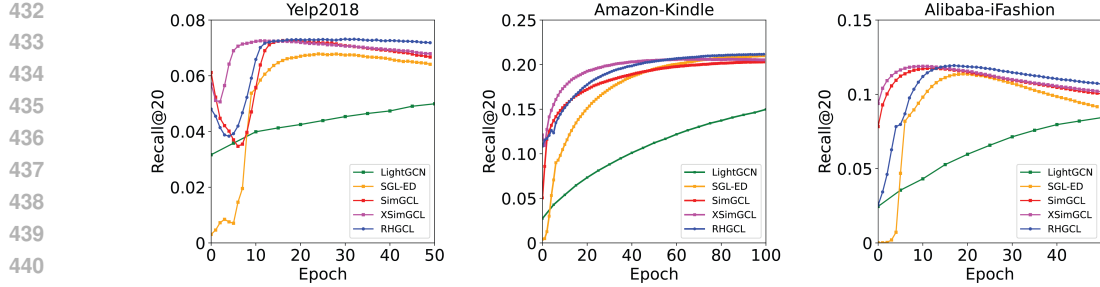
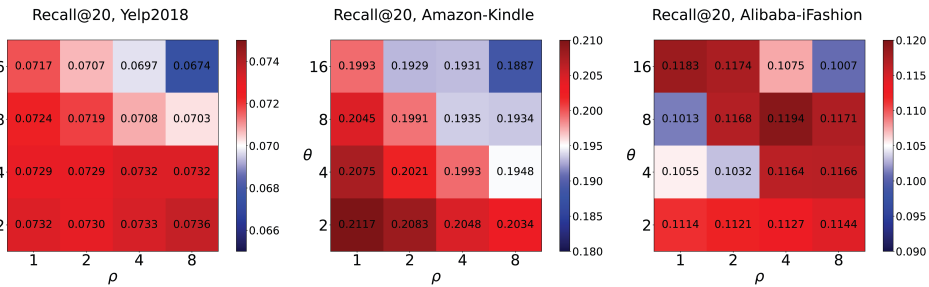


Figure 2: Learning curves of different models on the three datasets.

To analyze the training dynamics of different models, we visualize the evolution of Recall@20 scores in Fig. 2. We see that the learning curves of RHGCL exhibit a trend similar to that of SimGCL and XSimGCL. On the Yelp2018 dataset, the Recall@20 score of RHGCL first declines before subsequently increasing. For the Amazon-Kindle dataset, the score of RHGCL exhibits steady upward trend. Finally, there is an increasing-then-decreasing pattern on the Alibaba-iFashion dataset. Notably, RHGCL consistently achieves highest prediction accuracy. This can be reflected by its ability to (1) reach larger Recall@20 scores; and (2) sustain larger scores over a longer span of training epochs, particularly on the Yelp2018 dataset.

### 5.3 SENSITIVITY STUDY

In this subsection, we investigate the influence of the spatial division parameters  $\rho$  and  $\theta$  on prediction performance in Fig. 3. Recall that  $\rho$  and  $\theta$  denote the number of radial and angular divisions, respectively. The results show that setting  $\theta = 2$  on the Yelp2018 and Amazon-Kindle datasets yield optimal performance, whereas  $\theta = 8, \rho = 4$  leads to highest accuracy on the Alibaba-iFashion dataset. These findings suggest that the best hyperparameter settings are task-specific, depending on user-item interaction properties (Answer Q3). On one hand, increasing  $\rho$  and  $\theta$  results in a greater number of divisions and item clusters, enabling finer-grained item cluster modeling. On the other hand, a larger number of divisions may lead to more boundary-adjacent items and cut off item interactions across division sector boundaries.

Figure 3: Recall@20 scores from RHGCL with different values of hyperparameters  $\rho$  and  $\theta$ .

We also investigate the influence of perplexity, which measures the number of selected neighborhoods in the t-SNE algorithm, on recommendation performance. A higher value of perplexity implies that the algorithm considers a wider range of neighborhoods when projecting representations. As illustrated in Fig. 4, the perplexity setting of 30 yields the highest Recall@20 and NDCG@20 scores among the five tested values on the Yelp2018 and Alibaba-iFashion datasets. In contrast, the Recall@20 and NDCG@20 scores on the Amazon-Kindle dataset exhibit only moderate sensitivity to changes in perplexity. These findings suggest that tuning the perplexity parameter can be a viable strategy for enhancing recommendation when applying RHGCL to other datasets.

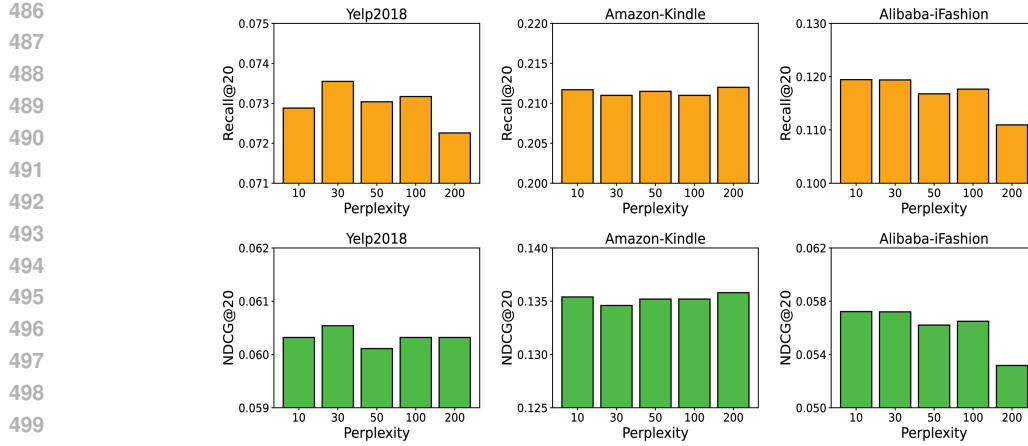


Figure 4: Recall@20 and NDCG@20 scores from RHGCL with different values of perplexity in t-SNE.

## 6 CONCLUSION

This study proposes a generalizable graph contrastive learning approach, called RHGCL, for user-item recommendation tasks. RHGCL performs contrastive learning on node representations during both the pre-training phase, utilizing the original user-item graph, and the fine-tuning phase, employing a two-hierarchy user-item bipartite graph. Note that our method functions as an extension of existing GCL methods, thereby ensuring high generalizability. Experimental results on three open user-item datasets confirm the positive contribution of hierarchical item structures and overall superior performance of RHGCL. One limitation of this study is that the superiority of our proposed RHGCL method has not been demonstrated on large-scale industrial recommendation datasets that contain over millions of user and item nodes. Future studies can explore the role of hierarchical item structures in such scenarios. **Moreover, the semantic interpretability of the clustered items is limited, due to the scarcity of item category information in the three datasets. This gap can be mitigated when datasets with richer categorical annotations are available.**

## 540 ACKNOWLEDGMENTS

541

542 This study is supported by our anonymous agencies.

543

## 544 THE USE OF LARGE LANGUAGE MODELS

545

546 We have employed Large Language Models to polish texts in this paper.

547

## 548 REFERENCES

549

550 Anirudhan Badrinath, Alex Yang, Kousik Rajesh, Prabhat Agarwal, Jaewon Yang, Haoyu Chen,  
551 Jiajing Xu, and Charles Rosenberg. OmniSage: Large scale, multi-entity heterogeneous graph  
552 representation learning. *ArXiv preprint arXiv:2504.17811*, 2025.

553

554 Paul Baltescu, Haoyu Chen, Nikil Pancha, Andrew Zhai, Jure Leskovec, and Charles Rosenberg.  
555 ItemSage: Learning product embeddings for shopping recommendations at Pinterest. In *Pro-  
556 ceedings of the 28th ACM SIGKDD Conference on Knowledge Discovery and Data Mining*, pp.  
2703–2711, 2022.

557

558 Fedor Borisyuk, Shihai He, Yunbo Ouyang, Morteza Ramezani, Peng Du, Xiaochen Hou, Cheng-  
559 ming Jiang, Nitin Pasumarthy, Priya Bannur, Birjodh Tiwana, et al. LiGNN: Graph neural net-  
560 works at LinkedIn. In *Proceedings of the 30th ACM SIGKDD Conference on Knowledge Discov-  
ery and Data Mining*, pp. 4793–4803, 2024.

561

562 Yuri M Brovman, Marie Jacob, Natraj Srinivasan, Stephen Neola, Daniel Galron, Ryan Snyder,  
563 and Paul Wang. Optimizing similar item recommendations in a semi-structured marketplace to  
564 maximize conversion. In *Proceedings of the 10th ACM Conference on Recommender Systems*,  
pp. 199–202, 2016.

565

566 Xuheng Cai, Chao Huang, Lianghao Xia, and Xubin Ren. LightGCL: Simple yet effective graph  
567 contrastive learning for recommendation. In *The Eleventh International Conference on Learning  
568 Representations*, 2023.

569

570 Hao Chen, Yuanchen Bei, Qijie Shen, Yue Xu, Sheng Zhou, Wenbing Huang, Feiran Huang, Sen-  
571 zhang Wang, and Xiao Huang. Macro graph neural networks for online billion-scale recommender  
572 systems. In *Proceedings of the ACM Web Conference 2024*, pp. 3598–3608, 2024a.

573

574 Jinsong Chen, Hanpeng Liu, John Hopcroft, and Kun He. Leveraging contrastive learning for en-  
575 hanced node representations in tokenized graph transformers. *Advances in Neural Information  
576 Processing Systems*, 37:85824–85845, 2024b.

577

578 Mengru Chen, Chao Huang, Lianghao Xia, Wei Wei, Yong Xu, and Ronghua Luo. Heterogeneous  
579 graph contrastive learning for recommendation. In *Proceedings of the Sixteenth ACM Interna-  
580 tional Conference on Web Search and Data Mining*, pp. 544–552, 2023.

581

582 Ting Chen, Simon Kornblith, Mohammad Norouzi, and Geoffrey Hinton. A simple framework for  
583 contrastive learning of visual representations. In *International Conference on Machine Learning*,  
pp. 1597–1607. PMLR, 2020.

584

585 James Davidson, Benjamin Liebald, Junning Liu, Palash Nandy, Taylor Van Vleet, Ullas Gargi,  
586 Sujoy Gupta, Yu He, Mike Lambert, Blake Livingston, et al. The YouTube video recommendation  
587 system. In *Proceedings of the Fourth ACM Conference on Recommender Systems*, pp. 293–296,  
2010.

588

589 Ningya Feng, Junwei Pan, Jialong Wu, Baixu Chen, Ximei Wang, Xian Hu, Jie Jiang, Mingsheng  
590 Long, et al. Long-sequence recommendation models need decoupled embeddings. In *The Thir-  
teenth International Conference on Learning Representations*, 2025.

591

592 Chen Gao, Yu Zheng, Nian Li, Yinfeng Li, Yingrong Qin, Jinghua Piao, Yuhan Quan, Jianxin Chang,  
593 Depeng Jin, Xiangnan He, et al. A survey of graph neural networks for recommender systems:  
Challenges, methods, and directions. *ACM Transactions on Recommender Systems*, 1(1):1–51,  
2023.

- 594 Ramin Giahi, Reza Yousefi Maragheh, Nima Farroksiar, Jianpeng Xu, Jason Cho, Evren Kor-  
 595 peoglu, Sushant Kumar, and Kannan Achan. GNN-GMVO: Graph neural networks for optimizing  
 596 gross merchandise value in similar item recommendation. In *2023 IEEE International Conference  
 597 on Data Mining Workshops (ICDMW)*, pp. 1484–1492. IEEE, 2023.
- 598 Xavier Glorot and Yoshua Bengio. Understanding the difficulty of training deep feedforward neural  
 599 networks. In *Proceedings of the Thirteenth International Conference on Artificial Intelligence  
 600 and Statistics*, pp. 249–256. JMLR Workshop and Conference Proceedings, 2010.
- 601 Jean-Bastien Grill, Florian Strub, Florent Altché, Corentin Tallec, Pierre Richemond, Elena  
 602 Buchatskaya, Carl Doersch, Bernardo Avila Pires, Zhaohan Guo, Mohammad Gheshlaghi Azar,  
 603 et al. Bootstrap your own latent-a new approach to self-supervised learning. *Advances in Neural  
 604 Information Processing Systems*, 33:21271–21284, 2020.
- 605 Xiaojun Guo, Yifei Wang, Zeming Wei, and Yisen Wang. Architecture matters: Uncovering implicit  
 606 mechanisms in graph contrastive learning. *Advances in Neural Information Processing Systems*,  
 607 36:28585–28610, 2023.
- 608 Will Hamilton, Zhitao Ying, and Jure Leskovec. Inductive representation learning on large graphs.  
 609 *Advances in Neural Information Processing Systems*, 30, 2017.
- 610 Kaveh Hassani and Amir Hosein Khasahmadi. Contrastive multi-view representation learning on  
 611 graphs. In *International Conference on Machine Learning*, pp. 4116–4126. PMLR, 2020.
- 612 Dongxiao He, Lianze Shan, Jitao Zhao, Hengrui Zhang, Zhen Wang, and Weixiong Zhang. Exploita-  
 613 tion of a latent mechanism in graph contrastive learning: Representation scattering. *Advances in  
 614 Neural Information Processing Systems*, 37:115351–115376, 2024.
- 615 Xiangnan He, Kuan Deng, Xiang Wang, Yan Li, Yongdong Zhang, and Meng Wang. LightGCN:  
 616 Simplifying and powering graph convolution network for recommendation. In *Proceedings of  
 617 the 43rd International ACM SIGIR Conference on Research and Development in Information  
 Retrieval*, pp. 639–648, 2020.
- 618 Tinglin Huang, Yuxiao Dong, Ming Ding, Zhen Yang, Wenzheng Feng, Xinyu Wang, and Jie Tang.  
 619 MixGCF: An improved training method for graph neural network-based recommender systems.  
 620 In *Proceedings of the 27th ACM SIGKDD Conference on Knowledge Discovery & Data Mining*,  
 621 pp. 665–674, 2021.
- 622 Wei Ju, Yifan Wang, Yifang Qin, Zhengyang Mao, Zhiping Xiao, Junyu Luo, Junwei Yang, Yiyang  
 623 Gu, Dongjie Wang, Qingqing Long, et al. Towards graph contrastive learning: A survey and  
 624 beyond. *ArXiv preprint arXiv:2405.11868*, 2024.
- 625 Wang-Cheng Kang and Julian McAuley. Self-attentive sequential recommendation. In *2018 IEEE  
 626 International Conference on Data Mining (ICDM)*, pp. 197–206. IEEE, 2018.
- 627 Diederik P. Kingma and Jimmy Ba. Adam: A method for stochastic optimization. *ArXiv preprint  
 628 arXiv:1412.6980*, 2014.
- 629 TN Kipf. Semi-supervised classification with graph convolutional networks. *ArXiv preprint  
 630 arXiv:1609.02907*, 2016.
- 631 Dongha Lee, SeongKu Kang, Hyunjun Ju, Chanyoung Park, and Hwanjo Yu. Bootstrapping user and  
 632 item representations for one-class collaborative filtering. In *Proceedings of the 44th International  
 633 ACM SIGIR Conference on Research and Development in Information Retrieval*, pp. 317–326,  
 634 2021.
- 635 Yakun Li, Lei Hou, Dongmei Li, and Juanzi Li. HKGCL: Hierarchical graph contrastive learning  
 636 for multi-domain recommendation over knowledge graph. *Expert Systems with Applications*, 233:  
 637 120963, 2023.
- 638 Zhao Li, Xin Shen, Yuhang Jiao, Xuming Pan, Pengcheng Zou, Xianling Meng, Chengwei Yao,  
 639 and Jiajun Bu. Hierarchical bipartite graph neural networks: Towards large-scale E-commerce  
 640 applications. In *2020 IEEE 36th International Conference on Data Engineering (ICDE)*, pp.  
 641 1677–1688. IEEE, 2020.

- 648 Dawen Liang, Rahul G Krishnan, Matthew D Hoffman, and Tony Jebara. Variational autoencoders  
 649 for collaborative filtering. In *Proceedings of the 2018 World Wide Web Conference*, pp. 689–698,  
 650 2018.
- 651 Xinyu Lin, Chaoqun Yang, Wenjie Wang, Yongqi Li, Cunxiao Du, Fuli Feng, See-Kiong Ng, and  
 652 Tat-Seng Chua. Efficient inference for large language model-based generative recommendation.  
 653 In *The Thirteenth International Conference on Learning Representations*, 2025.
- 654 Zihan Lin, Changxin Tian, Yupeng Hou, and Wayne Xin Zhao. Improving graph collaborative filter-  
 655 ing with neighborhood-enriched contrastive learning. In *Proceedings of the ACM Web Conference*  
 656 2022, pp. 2320–2329, 2022.
- 657 Aaron van den Oord, Yazhe Li, and Oriol Vinyals. Representation learning with contrastive predic-  
 658 tive coding. *ArXiv preprint arXiv:1807.03748*, 2018.
- 659 Yingrong Qin, Chen Gao, Shuangqing Wei, Yue Wang, Depeng Jin, Jian Yuan, Lin Zhang, Dong Li,  
 660 Jianye Hao, and Yong Li. Learning from hierarchical structure of knowledge graph for recom-  
 661 mendation. *ACM Transactions on Information Systems*, 42(1):1–24, 2023.
- 662 Steffen Rendle, Christoph Freudenthaler, Zeno Gantner, and Lars Schmidt-Thieme. BPR: Bayesian  
 663 personalized ranking from implicit feedback. *ArXiv preprint arXiv:1205.2618*, 2012.
- 664 Joshua Robinson, Rishabh Ranjan, Weihua Hu, Kexin Huang, Jiaqi Han, Alejandro Dobles, Matthias  
 665 Fey, Jan Eric Lenssen, Yiwen Yuan, Zecheng Zhang, et al. Relational deep learning: Graph  
 666 representation learning on relational databases. In *NeurIPS 2024 Third Table Representation*  
 667 *Learning Workshop*, 2024.
- 668 Changsheng Shui, Xiang Li, Jianpeng Qi, Guiyuan Jiang, and Yanwei Yu. Hierarchical graph con-  
 669 trastive learning for review-enhanced recommendation. In *Joint European Conference on Ma-*  
 670 *chine Learning and Knowledge Discovery in Databases*, pp. 423–440. Springer, 2024.
- 671 Laurens Van Der Maaten. Barnes-hut-sne. *ArXiv preprint arXiv:1301.3342*, 2013.
- 672 Laurens Van der Maaten and Geoffrey Hinton. Visualizing data using t-SNE. *Journal of Machine*  
 673 *Learning Research*, 9(11), 2008.
- 674 Petar Veličković, William Fedus, William L Hamilton, Pietro Liò, Yoshua Bengio, and R Devon  
 675 Hjelm. Deep graph infomax. *ArXiv preprint arXiv:1809.10341*, 2018.
- 676 Andrew Z Wang, Rex Ying, Pan Li, Nikhil Rao, Karthik Subbian, and Jure Leskovec. Bipartite dy-  
 677 namic representations for abuse detection. In *Proceedings of the 27th ACM SIGKDD Conference*  
 678 *on Knowledge Discovery & Data Mining*, pp. 3638–3648, 2021a.
- 679 Ke Wang, Yanmin Zhu, Tianzi Zang, Chunyang Wang, and Mengyuan Jing. Review-enhanced  
 680 hierarchical contrastive learning for recommendation. In *Proceedings of the AAAI Conference on*  
 681 *Artificial Intelligence*, volume 38, pp. 9107–9115, 2024.
- 682 Xiang Wang, Xiangnan He, Meng Wang, Fuli Feng, and Tat-Seng Chua. Neural graph collabora-  
 683 tive filtering. In *Proceedings of the 42nd International ACM SIGIR Conference on Research and*  
 684 *Development in Information Retrieval*, pp. 165–174, 2019.
- 685 Xiao Wang, Nian Liu, Hui Han, and Chuan Shi. Self-supervised heterogeneous graph neural network  
 686 with co-contrastive learning. In *Proceedings of the 27th ACM SIGKDD Conference on Knowledge*  
 687 *Discovery & Data Mining*, pp. 1726–1736, 2021b.
- 688 Hongjie Wei, Junli Wang, Yu Ji, Mingjian Guang, and Chungang Yan. Hierarchical neighbor-  
 689 enhanced graph contrastive learning for recommendation. *Knowledge-Based Systems*, 315:  
 690 113263, 2025.
- 691 Jiancan Wu, Xiang Wang, Fuli Feng, Xiangnan He, Liang Chen, Jianxun Lian, and Xing Xie. Self-  
 692 supervised graph learning for recommendation. In *Proceedings of the 44th International ACM*  
 693 *SIGIR Conference on Research and Development Information Retrieval*, pp. 726–735, 2021a.

- 702 Zhanghao Wu, Paras Jain, Matthew Wright, Azalia Mirhoseini, Joseph E Gonzalez, and Ion Stoica.  
 703 Representing long-range context for graph neural networks with global attention. *Advances in*  
 704 *Neural Information Processing Systems*, 34:13266–13279, 2021b.
- 705 Lianghao Xia, Chao Huang, Yong Xu, Jiashu Zhao, Dawei Yin, and Jimmy Huang. Hypergraph con-  
 706 trastive collaborative filtering. In *Proceedings of the 45th International ACM SIGIR Conference*  
 707 *on Research and Development in Information Retrieval*, pp. 70–79, 2022.
- 708 Teng Xiao, Huaisheng Zhu, Zhengyu Chen, and Suhang Wang. Simple and asymmetric graph  
 709 contrastive learning without augmentations. *Advances in Neural Information Processing Systems*,  
 710 36:16129–16152, 2023.
- 711 Dongkuan Xu, Wei Cheng, Dongsheng Luo, Haifeng Chen, and Xiang Zhang. InfoGCL:  
 712 Information-aware graph contrastive learning. *Advances in Neural Information Processing Sys-*  
 713 *tems*, 34:30414–30425, 2021a.
- 714 Minghao Xu, Hang Wang, Bingbing Ni, Hongyu Guo, and Jian Tang. Self-supervised graph-level  
 715 representation learning with local and global structure. In *International Conference on Machine*  
 716 *Learning*, pp. 11548–11558. PMLR, 2021b.
- 717 Hao Yan, Senzhang Wang, Jun Yin, Chaozhuo Li, Junxing Zhu, and Jianxin Wang. Hierarchical  
 718 graph contrastive learning. In *Joint European Conference on Machine Learning and Knowledge*  
 719 *Discovery in Databases*, pp. 700–715. Springer, 2023.
- 720 Haoran Yang, Xiangyu Zhao, Yicong Li, Hongxu Chen, and Guandong Xu. An empirical study to-  
 721 wards prompt-tuning for graph contrastive pre-training in recommendations. *Advances in Neural*  
 722 *Information Processing Systems*, 36:62853–62868, 2023.
- 723 Tiansheng Yao, Xinyang Yi, Derek Zhiyuan Cheng, Felix Yu, Ting Chen, Aditya Menon, Lichan  
 724 Hong, Ed H Chi, Steve Tjoa, Jieqi Kang, et al. Self-supervised learning for large-scale item  
 725 recommendations. In *Proceedings of the 30th ACM International Conference on Information &*  
 726 *Knowledge Management*, pp. 4321–4330, 2021.
- 727 Rex Ying, Ruining He, Kaifeng Chen, Pong Eksombatchai, William L Hamilton, and Jure Leskovec.  
 728 Graph convolutional neural networks for web-scale recommender systems. In *Proceedings of the*  
 729 *24th ACM SIGKDD International Conference on Knowledge Discovery & Data Mining*, pp. 974–  
 730 983, 2018a.
- 731 Zhitao Ying, Jiaxuan You, Christopher Morris, Xiang Ren, Will Hamilton, and Jure Leskovec. Hier-  
 732 archical graph representation learning with differentiable pooling. *Advances in Neural Infor-*  
 733 *mation Processing Systems*, 31, 2018b.
- 734 Yuning You, Tianlong Chen, Yongduo Sui, Ting Chen, Zhangyang Wang, and Yang Shen. Graph  
 735 contrastive learning with augmentations. *Advances in Neural Information Processing Systems*,  
 736 33:5812–5823, 2020.
- 737 Junliang Yu, Hongzhi Yin, Xin Xia, Tong Chen, Lizhen Cui, and Quoc Viet Hung Nguyen. Are  
 738 graph augmentations necessary? Simple graph contrastive learning for recommendation. In *Pro-*  
 739 *ceedings of the 45th International ACM SIGIR Conference on Research and Development in In-*  
 740 *formation Retrieval*, pp. 1294–1303, 2022.
- 741 Junliang Yu, Xin Xia, Tong Chen, Lizhen Cui, Nguyen Quoc Viet Hung, and Hongzhi Yin.  
 742 XSimGCL: Towards extremely simple graph contrastive learning for recommendation. *IEEE*  
 743 *Transactions on Knowledge and Data Engineering*, 36(2):913–926, 2023a.
- 744 Junliang Yu, Hongzhi Yin, Xin Xia, Tong Chen, Jundong Li, and Zi Huang. Self-supervised learning  
 745 for recommender systems: A survey. *IEEE Transactions on Knowledge and Data Engineering*,  
 746 36(1):335–355, 2023b.
- 747 Meng Yuan, Zhao Zhang, Wei Chen, Chu Zhao, Tong Cai, Deqing Wang, Rui Liu, and Fuzhen  
 748 Zhuang. HEK-CL: Hierarchical enhanced knowledge-aware contrastive learning for recom-  
 749 *commendation. ACM Transactions on Information Systems*, 2025a.

- 756 Yiwen Yuan, Zecheng Zhang, Xinwei He, Akihiro Nitta, Weihua Hu, Dong Wang, Manan Shah,  
757 Shenyang Huang, Blaž Stojanovič, Alan Krumholz, Jan Eric Lenssen, Jure Leskovec, and  
758 Matthias Fey. ContextGNN: Beyond two-tower recommendation systems. In *Thirteenth Interna-*  
759 *tional Conference on Learning Representations*, 2025b.
- 760
- 761 Qian Zhao, Zhengwei Wu, Zhiqiang Zhang, and Jun Zhou. Long-tail augmented graph contrastive  
762 learning for recommendation. In *Joint European Conference on Machine Learning and Knowl-*  
763 *edge Discovery in Databases*, pp. 387–403. Springer, 2023.
- 764
- 765 Yanqiao Zhu, Yichen Xu, Feng Yu, Qiang Liu, Shu Wu, and Liang Wang. Deep graph contrastive  
766 representation learning. *ArXiv preprint arXiv:2006.04131*, 2020.
- 767
- 768
- 769
- 770
- 771
- 772
- 773
- 774
- 775
- 776
- 777
- 778
- 779
- 780
- 781
- 782
- 783
- 784
- 785
- 786
- 787
- 788
- 789
- 790
- 791
- 792
- 793
- 794
- 795
- 796
- 797
- 798
- 799
- 800
- 801
- 802
- 803
- 804
- 805
- 806
- 807
- 808
- 809

810  
811  
812  
813  
814 A COMPARISON WITH EXISTING STUDIES  
815  
816  
817  
818  
819  
820  
821  
822813  
814 Table 3: Comparison between our model and recent studies on hierarchical graph contrastive learn-  
815 ing for recommendation systems. U-I: User-Item. KGs: Knowledge Graphs. U-U: User-User. I-I:  
816 Item-Item.

Study	Target	Graph learning	Contrastive learning	Hierarchy
HKGCL (Li et al., 2023)	U-I ratings	Along KGs	Cross domains	From domains
HGCL (Shui et al., 2024)	U-I ratings	Along subgraphs	Cross subgraphs	From node neighbors
ReHCL (Wang et al., 2024)	U-I ratings	Along topic&semantic graphs	Cross-views&cross-modal	From review text data
HEK-CL (Yuan et al., 2025a)	U-I interactions	Along KGs	Cross graphs and KGs	From KGs
HNECL (Wei et al., 2025)	U-I interactions	Along U-I, U-U, I-I graphs	Cross layers	From two-hop neighbors
RHGCL	U-I interactions	Along U-I graphs	Cross layers	From entire graphs

823  
824 We summarize recent hierarchical GCL approaches for recommendation systems in Table 3 to clarify  
825 the distinctions between our proposed RHGCL models and recent methods. In particular, recent  
826 models can be categorized into three types.

- **Incorporating KGs.** HKGCL (Li et al., 2023) conducts graph learning based on edges within KGs, whereas HEK-CL (Yuan et al., 2025a) develops its contrastive learning module by leveraging the structural properties of KGs. The two models are effective when the external item-relationship data is available to construct KGs. In contrast, our approach relies on only U-I interactions, which are generally more accessible.
- **Utilizing review data.** ReHCL (Wang et al., 2024) employs review data—which contains rich semantic information from users regarding items—to conduct hierarchical GCL on U-I ratings. While useful, the availability of user review data is sometimes limited, often due to issues such as privacy considerations.
- **Relying on node neighbors.** The models HGCL (Shui et al., 2024) and HNECL (Wei et al., 2025) establish hierarchical structures for contrastive learning by exploiting node neighborhood relationships. Different from the two models, our proposed RHGCL model derives hierarchical structures by clustering node representations across the entire set of items, thereby enabling a more comprehensive capture of global item-level information.

842  
843 B DATASETS  
844

845 We use the following three datasets to examine the performance of RHGCL.

- **Yelp2018. training set:** 31,668 users; 38,048 items (i.e., local business); 1,237,259 user-item interactions. **testing set:** 31,668 users; 36,073 items; 324,147 user-item interactions.
- **Amazon-Kindle. training set:** 138,333 users; 98,572 items (i.e., books); 1,527,913 interactions. **testing set:** 107,593 users; 82,935 items; 382,052 interactions.
- **Alibaba-iFashion. training set:** 300,000 users; 81,614 items (i.e., garments); 1,255,447 interactions; **testing set:** 268,847 users; 48,483 items; 352,366 interactions.

854  
855 C BASELINE MODELS  
856857 The **eight** baseline models are listed below.

- **BUIR** is a two-encoder representation framework without negative sampling (Lee et al., 2021).
- **DNN+SSL** employs data augmentation methods to handle data sparsity problems (Yao et al., 2021).
- **LightGCN** represents a streamlined version of GNNs, removing linear transformation and nonlinear activation operations (He et al., 2020).

- **NCL** incorporates the potential neighbors of a node from structural and semantic spaces into contrastive learning (Lin et al., 2022).
- **SGL** introduces self-supervision into graph learning by leveraging multiple views derived from the original user-item graphs (Wu et al., 2021a).
- **SimGCL** enhances SGL by adding random noises during the model training process (Yu et al., 2022).
- **XSimGCL** simplifies SimGCL by unifying graph-based recommendation and contrastive learning into a single information propagation (Yu et al., 2023a).
- **HNECL** clusters node embeddings into hierarchical prototypes and conducts contrastive learning between user and item embeddings across distinct graph convolution layers (Wei et al., 2025).

## D CONNECTING STRENGTH ANALYSIS

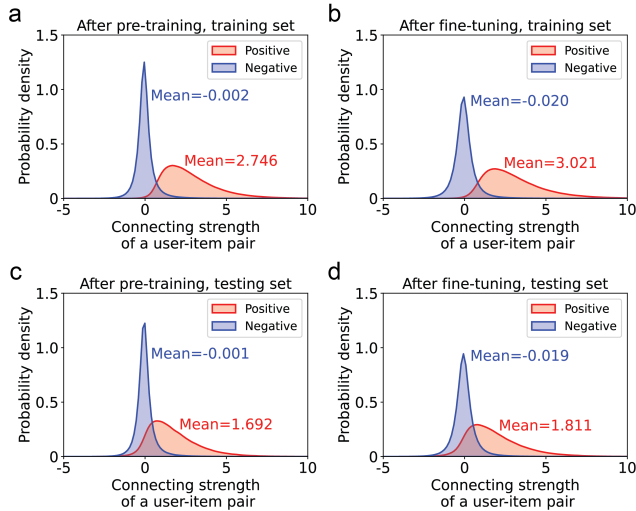


Figure 5: The connecting strength of positive and negative user-item pairs after pre-training (a, c) and fine-tuning (b, d) on the Yelp2018 dataset.

To further validate the contribution of the item clustering and fine-tuning modules in RHGCL, we track the changes in the connection strength of user-item pairs. As described in Sec. 3.1, the connecting strength (i.e.,  $\hat{y}_{ij}$ ) is defined as the dot product between the representations of user  $i$  and item  $j$ , where a higher value of  $\hat{y}_{ij}$  corresponds to an increased probability of recommendation.

We visualize the probability density distribution of the connecting strength for positive and negative user-item pairs on the Yelp2018 dataset in Fig. 5. Here, positive pairs refer to user-item pairs observed in the training or testing sets. Negative pairs are generated by randomly sampling ten items from the entire item set for each user in the training or testing sets. Note that Fig. 5a and b correspond to the training set, whereas Fig. 5c and d correspond to the testing set. Comparing Fig. 5a and b, we can see that the average connecting strength increases from 2.746 to 3.021 for the positive user-item pairs, and decreases from -0.002 to -0.020 for the negative user-item pairs. These changes indicate that positive pairs are more distinguishable with negative pairs after fine-tuning than after pre-training. Similarly, on the testing set (Fig. 5c and d), we observe an increase of average connecting strength for positive edges (from 1.692 to 1.811) and a decrease of average connecting strength for negative edges (from -0.001 to -0.019). All these results provide strong empirical evidence that our designed item clustering and fine-tuning modules in RHGCL effectively enhance the recommendation performance.

918 E TIME COMPLEXITY ANALYSIS  
919

920 In this section, we present the time complexity analysis of our proposed RHGCL and contrast it with  
921 XSimGCL. To clarify, we first summarize key notations. Recall from Sec. 3 that  $|\mathcal{E}|$  represents the  
922 number of edges in the user-item bipartite graph.  $K$  is the number of layers in graph convolution op-  
923 erations and  $d$  represents the node embedding dimension. We introduce  $|\mathcal{E}^{uc}|$  to denote the number  
924 of edges between the user set  $\mathcal{U}$  and the clustered item set  $\mathcal{C}$ . Hence, we have:

$$925 \quad |\mathcal{E}^{uc}| \leq |\mathcal{E}|, |\mathcal{E}^{uc}| \leq m\rho\theta. \quad (9)$$

927 The first inequality holds since each user-item pair in  $\mathcal{E}$  is mapped to a user-clustered item pair in  
928  $\mathcal{E}^{uc}$ . The second inequality follows from the fact that the number of edges in  $\mathcal{U} \cup \mathcal{C}$  is upper bounded  
929 by the size of  $\mathcal{U}$  (i.e.,  $m$ ) and the size of  $\mathcal{C}$  (i.e.,  $\rho\theta$ ). Further, we use  $b$  to represent the batch size and  
930  $B$  to denote the number of nodes within a batch.

931  
932 Table 4: Time complexity comparison between XSimGCL and RHGCL.

933 Model	934 Graph convolution	935 Recommendation loss	936 Contrastive loss
XSimGCL	$\mathcal{O}(2 \mathcal{E} Kd)$	$\mathcal{O}(2bd)$	$\mathcal{O}(bBd)$
RHGCL	$\mathcal{O}(2 \mathcal{E} Kd) + \mathcal{O}(2 \mathcal{E}^{uc} Kd)$	$\mathcal{O}(2bd)$	$\mathcal{O}(bBd)$

937 Accordingly, we summarize the time complexity of RHGCL and XSimGCL in Table 4. Recall  
938 from Sec. 4.3 that we perform graph convolution operations on the user-item graph and the user-  
939 clustered item graph separately. This introduces an additional graph convolution time complexity  
940  $\mathcal{O}(2|\mathcal{E}^{uc}|Kd)$ , which is theoretically upper bounded by  $\mathcal{O}(2|\mathcal{E}|Kd)$  and is empirically small given  
941 the small number of clusters (i.e.,  $\rho\theta$ ). Moreover, the time complexity of the recommendation loss  
942 calculation in RHGCL scales linearly with both  $b$  and  $d$ , which is the same as those from XSimGCL.  
943 Recall from Sec. 4.3 that the contrastive loss is computed over  $\mathcal{U}$  and  $\mathcal{I}$ , leading to the same time  
944 complexity  $\mathcal{O}(bBd)$  as XSimGCL. Together, RHGCL introduces only a minor increase in time  
945 complexity over XSimGCL.  
946  
947  
948  
949  
950  
951  
952  
953  
954  
955  
956  
957  
958  
959  
960  
961  
962  
963  
964  
965  
966  
967  
968  
969  
970  
971